In-Situ Synthesis and Characterization of TiB₂ and Ti-Al-B Composites

Muralidharan Ramachandran[1,#], Ramana G Reddy[1,*]

[1]Department of Metallurgical and Materials Engineering
The University of Alabama, Tuscaloosa, AL-35487, USA
[#]Current Address: Department of Metallurgical and Materials Engineering
National Institute of Technology (NIT), Trichy-620015, INDIA
*Corresponding Author

Keywords: TiB₂, SHS, Composites

Abstract

A facile self-propagating high-temperature synthesis (SHS) method for the synthesis of titanium diboride and Ti-Al-B composites are reported. In this one-step process, single-phase titanium diboride (TiB₂) is formed without the presence of TiB and Ti₃B₄. Porous titanium diboride with particle sizes ranging between 10 and 20 μm is formed. Crystallite size and lattice constants were calculated and compared with the literature. High temperatures of the exothermic reaction lead to consolidation of TiB₂ particles and grain growth. TiAl-TiB₂ composites were made in similar one-step synthesis procedure. Small amount of Ti₃Al was observed in addition to TiAl and TiB₂. The composites were heat-treated and analyzed for microstructure and hardness.

Introduction

Advanced materials with enhanced properties are of immense interest due to their potential in both extremely high and low temperatures; high pressure and vacuum conditions; corrosive environments, etc. Titanium diboride exhibits excellent properties such as high melting point of 3498±20 K[1], Vickers indentation hardness of 25 GPa (at 5 N load), and electrical and thermal conductivities of ~10^7 S/m and 96 W/m.K, respectively, at 298 K [2]. The corrosion and chemical resistance in various media, even at elevated temperatures, is much greater for titanium diboride, along with its superior wear resistant properties[3]. The binary phase diagram of Ti-B system is shown in Figure 1[4]. It is seen that TiB₂ is the highest melting temperature ceramic in the Ti-B system and is much more stable than TiB.

The synthesis of titanium diboride has been researched using various techniques. Electrodeposition from cryolite-based electrolytes at 960ºC and KF-KCl melts at 800ºC [5], induction plasma [6], plasma spray synthesis [7], self-propagating high-temperature synthesis (SHS) of titanium and boron carbide (B₄C) [8], reactive thermal spray [9], and spark plasma synthesis (SPS) [10] are some of the synthesis methods reported for titanium diboride. The synthesis of titanium diboride from TiO₂, B₂O₃ and CH₄ using thermal plasma synthesis technique has been reported in the literature [11]. The production of TiB₂ using thermal plasma has been carried out earlier by other researchers from ilmenite concentrates [12] and from TiO₂ and B₂O₃[13].
In this work, a one-step, self-propagating high-temperature synthesis (SHS) of titanium diboride is reported from elemental titanium and boron.
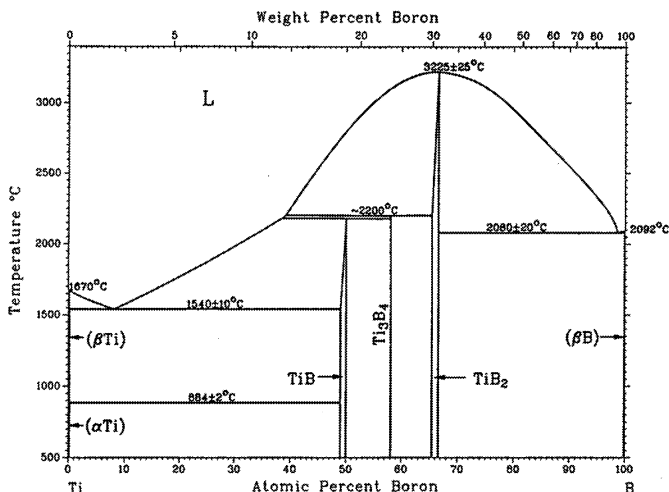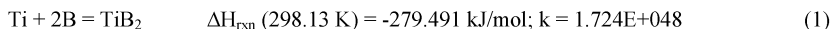
Figure 1: Ti-B binary phase diagram. (Reproduced with permission from Lu et al. [4], Kluwer Academic Publishers)

Theoretical

The heat of reaction for the formation of titanium diboride from elemental titanium and boron powders was calculated using HSC Chemistry 5.11® [14]. The reaction along with the exothermic heat (ΔH_{rxn} @ 298 K) and equilibrium constant, k are given in equation (1).

$$Ti + 2B = TiB_2 \qquad \Delta H_{rxn} (298.13 \text{ K}) = -279.491 \text{ kJ/mol; k} = 1.724E+048 \qquad (1)$$

According to equation 1, the formation of titanium diboride is extremely favorable and is an exothermic reaction. The experimental setup in this research is setup to provide the initial arc (heat) to start the self-propagating synthesis.

The synthesis of Ti-Al-B composite was also carried out using similar procedure. The corresponding reaction is reported in equation (2). It is observed that the formation of composite has more heat of reaction compared to that of formation of titanium diboride.

$$2Ti + Al + 2B = TiAl + TiB_2 \ \Delta H_{rxn} (298.13 \text{ K}) = -352.293 \text{ kJ/mol; k} = 4.390E+060 \qquad (2)$$
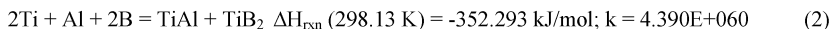
Experimental

The synthesis of titanium diboride (TiB_2) was carried out using elemental titanium (Alfa Aesar, 99%, ~325 mesh) and elemental boron (Alfa Aesar, crystalline, 98%, ~325 mesh). Stoichiometric quantities of elemental titanium and boron powders were mixed thoroughly. Elemental aluminum powders (Alfa Aesar, 99%, ~325 mesh) was used along with Ti and B powders for the synthesis of Ti-Al-B composites. The powders were made into pellets of diameter, 13 mm or 34 mm using a uniaxial pressure of about 25,000 psi.

The pellet was placed in an arc melter, a schematic of which is shown in Figure 2, on a water-cooled copper hearth under vacuum. Under partial argon pressure, an arc was struck from the plasma arc electrode to one end of the sample using a current of 200 A. Once the temperature of the sample reached the formation temperature of titanium diboride, the reaction self-propagated and the entire pellet was converted to TiB_2. In the case of Ti-Al-B composite, $TiAl-TiB_2$ was formed by similar self-propagation synthesis method.

Titanium diboride, thus formed, was crushed and analyzed for phases using X-Ray diffraction (XRD), model Phillips MPD (more details). Morphological analysis was carried out using scanning electron microscope (SEM), model Phillips XL30, equipped with energy dispersive spectrometer (EDS) and using transmission electron microscope (TEM), model Technai F-20.

The composite, $TiAl-TiB_2$, was heat treated at 900ºC for 120 hours to obtain homogenous material. The pellets after synthesis were wrapped individually in tantalum foil. Each of the wrapped pellets was sealed in a quartz tube under vacuum. The surface of the pellets was ground after heat treatment and analyzed using XRD and SEM for phase and morphology and subsequently for hardness.
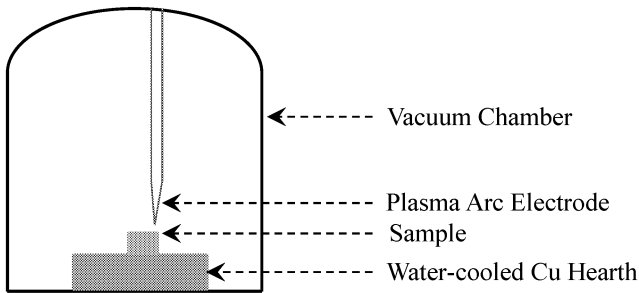

Figure 2: Experimental Setup for Synthesis of TiB₂.

Results and Discussion

The titanium diboride formed from SHS was crushed and analyzed using XRD. The powder XRD pattern shown in Figure 3 demonstrates the formation of phase pure hexagonal titanium diboride confirmed by the matching PCPDF# 04-015-0274 [15]. The XRD pattern also confirms the absence of other diborides such as the unstable TiB or Ti_3B_4 (as seen from Figure 1) during synthesis. The lattice constants, a and c, for the hexagonal lattice were calculated using equation (3).

$$1/_{d^2} = 4/_3 \left(h^2 + hk + k^2/_{a^2} \right) + l^2/_{c^2} \tag{3}$$

d is the spacing between two hkl planes.

Lattice constants were calculated for titanium diboride using two strong peaks corresponding to (101) and (100) planes samples obtained from two similar experiments. The value of a and c obtained were 3.0275±0.0073 Å and 3.2264±0.0081 Å, respectively. This is in very close agreement with the lattice parameters reported in the PCPDF# 04-015-0274, a = 3.0300(10)Å and c = 3.2280(20)Å.

Figure 3: XRD pattern of titanium diboride.

Figure 4: XRD pattern of TiAl-TiB$_2$ composite.

The XRD pattern of TiAl-TiB$_2$ composite shown in Figure 4 demonstrates the formation both the phases TiAl and TiB$_2$ as confirmed by the PCPDF files 04-006-6741 and 04-015-0274 [15], respectively. There are also small quantities of Ti$_3$Al that was observed in the XRD pattern matched using PCPDF# 04-008-5580. This is attributed to the loss of boron during the high temperature synthesis. The loss of boron leads to an increase in the amount of available titanium in the pellet leading to the formation of small quantities of Ti$_3$Al along with TiAl.

Lattice constants for TiB_2 in the $TiAl$-TiB_2 composite were calculated using equation (3) for hexagonal crystal lattice. The values of a and c obtained samples from six different experiments are 3.0269±0.0007 Å and 3.2313±0.0013 Å. Similar to TiB_2 experiments, the lattice parameters are in very close agreement with that reported in the PCPDF# 04-015-0274, a = 3.0300(10)Å and c = 3.2280(20)Å.
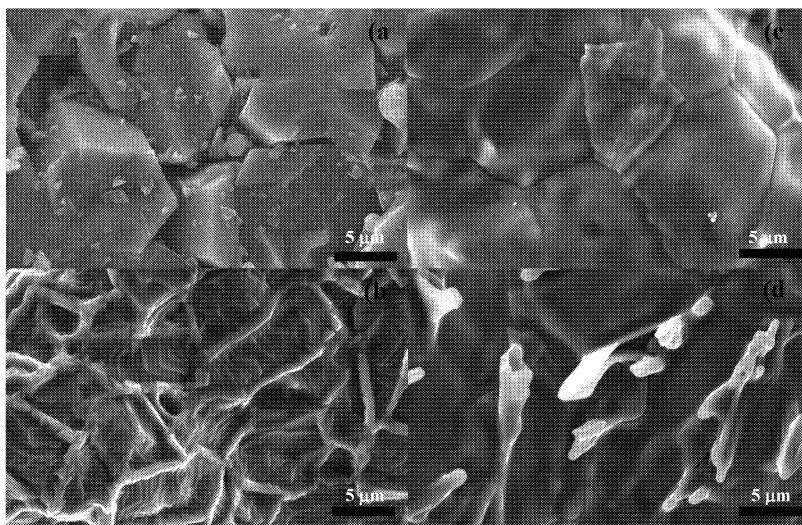

Figure 5: SEM images of titanium diboride synthesized using SHS (a) crushed powder; (b) top of uncrushed pellet; (c) and (d) bottom of uncrushed pellet.

Crystallite size of titanium diboride was calculated using Scherrer's equation: $L = k\lambda/(\beta_{1/2}\, cos\theta)$. L is the crystallite size; k is a constant, taken as 0.94, assuming spherical crystallites; λ is the wavelength of X-Ray radiation in Å; $\beta_{1/2}$ is the full width at half maxima (FWHM); and θ is the diffraction angle. The value of crystallite size obtained was 3.23 ± 0.53Å. The crystallite size of titanium diboride formed in the $TiAl$-TiB_2 composite was of same order of magnitude.

The crushed titanium diboride powders were analyzed using SEM for morphological analysis shown in Figure 5(a). The morphology shows hexagonal particles of approximately 15-20 μm in size. The temperature of the reaction is high enough for the titanium diboride particles to form faceted structure. The bigger particle sizes in comparison with the smaller crystallite sizes shows that nucleation of titanium diboride occurs with subsequent consolidation to form bigger particles. It is also important to report that the titanium diboride pellet formed was porous in nature. This could possibly be due to poor compaction of the starting materials and the reduction in volume of the pellet due to reaction. The volume of the reactants (Ti + 2B) is 10.630 ml/mol + 9.239 ml/mol = 19.869 ml, while the product (TiB_2) formed has a volume of 15.872 ml/mol.

Figure 5(b) shows the top surface of an uncrushed titanium diboride pellet after synthesis with average particle sizes of about 10 μm. The pellet during SHS is red-hot. The heat from the surface of the pellet is transferred to air which is at ambient temperature and sub-ambient pressure. The high temperature and the extreme temperature difference leads to enhanced grain growth. This is proven by the enhanced growth at the grain boundaries from the micrograph. The transfer of heat from the pellet to air might also provide a quenching effect decreasing the average particle size. The bottom of the uncrushed pellet, shown in Figures 5 (c) and (d), show the average particle sizes of about 10 μm, similar to the top surface but comparatively smaller than the bulk. This is probably due to the presence of the water-cooled copper plate that provides a quenching effect. In addition, some parts of the titanium diboride material from the bottom surface are protruded outward towards the water-cooled hearth. The direction of heat transfer causes this protrusion of material and is observed only near the water-cooled surface.
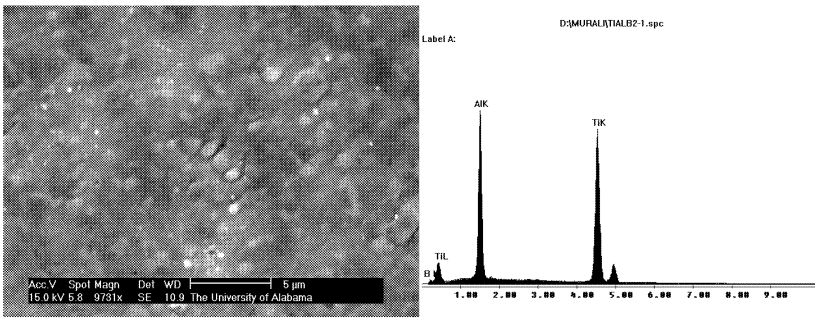

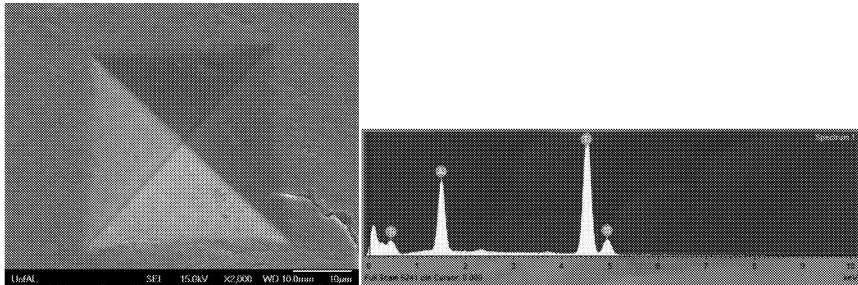Figure 6: SEM image of TiAl-TiB₂ composite and its corresponding EDS spectrum.

Figure 7: SEM image of Vicker's micro hardness indentation of TiAl-TiB₂ and its corresponding EDS spectrum.

The SEM image of TiAl-TiB₂ composite is shown in Figure 6. As can be seen from the image, TiB₂, with its 50 mol% in the composite, is evenly dispersed in TiAl. The EDS spectrum shows the presence of Ti, Al and B even though the presence of B is not reliable using EDS. Figure 7 shows Vicker's micro hardness indentation in the TiAl-TiB₂ composite and its corresponding EDS spectrum. Vicker's micro hardness was measured with a load of 1000 gf and a load time of 15 s. The micro hardness measured on the composite material using five different samples was 8.17±0.17 GPa.
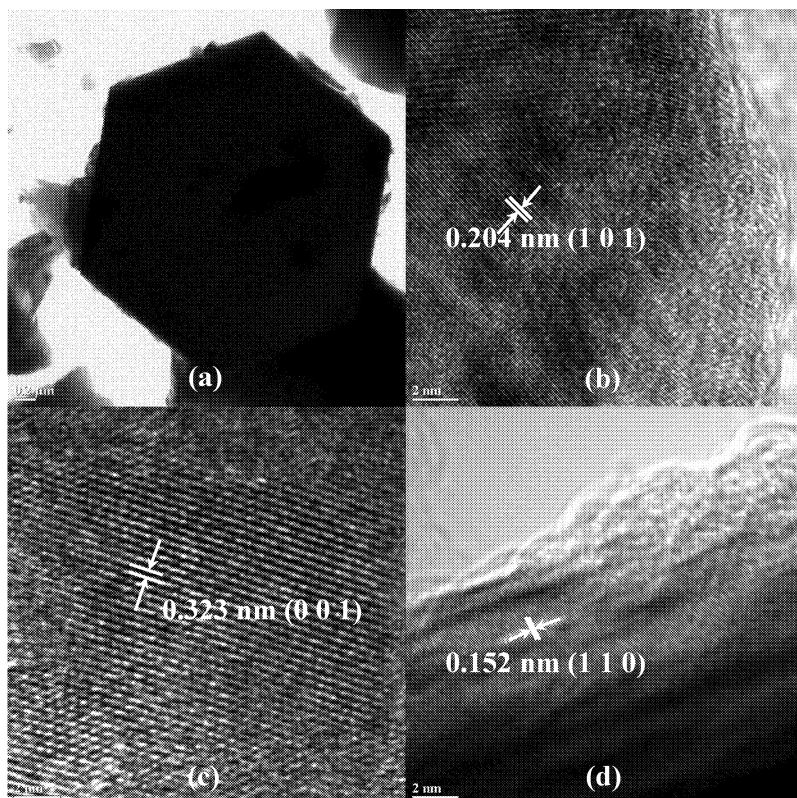
Figure 8: TEM image of titanium diboride (a); High-Resolution TEM images of titanium diboride (b), (c), and (d).

Transmission electron microscope (TEM) images of titanium diboride, synthesized using SHS, were obtained. Figure 8 (a) shows a hexagonal titanium diboride particle of about 2.5 μm in size. Even though the particle size determined using SEM shows a distribution between 15 and 20 μm, there are some smaller particles formed. High resolution images of TiB_2 are shown in Figure(s) 8 (b), (c), and (d). The d-spacing measurement of 0.204 nm, 0.323 nm, and 0.152 nm corresponding to (1 0 1), (0 0 1), and (1 1 0) of titanium diboride (PDF# 04-015-0274) show that the particles are polycrystalline.

Conclusions

A facile SHS method using arc melter was successfully employed in the synthesis of titanium diboride and $TiAl$-TiB_2 composite. Single-phase titanium diboride was formed with no other titanium borides such as TiB or Ti_3B_4 in the product. The average particle size varied between 10 - 20 μm. The exothermic reaction produced temperatures high enough for consolidation of the powders with the formation of faceted particles. The polycrystalline nature of the particles is observed from the lattice fringes in various orientations. The synthesis of in-situ composites was

successfully carried out using similar procedure for which the heat was provided by the exothermic reaction between Ti and B. XRD shows formation of TiAl and TiB_2 along with small quantities of Ti_3Al. SEM images show even distribution of TiB_2 in TiAl. Hardness measurements of the composite using Vicker's hardness were determined to be 8.17 ± 0.17 GPa.

References

1. H. Duschanek, P.R., and H. L. Lukas, *A critical assessment and thermodynamic calculation of the boron-carbon-titanium (B-C-Ti) ternary system.* Journal of Phase Equilibria, 1995. **16**(1): p. 46-60.
2. Munro, R.G., *Material Properties of Titanium Diboride.* Journal of Research of the National Institute of Standards and Technology, 2000. **105**(5): p. 709-720.
3. Blaise Champagne, S.D., *TiB.sub.2 -based materials and process of producing the same.* 1987, National Research Council Of Canada; Canadian Patents And Development Limited: US.
4. Lu, L., Lai, M. O., Wang, H. Y., *Synthesis of titanium diboride TiB2 and Ti-Al-B metal matrix composites.* Journal of Materials Science, 2000. **35**: p. 241-248.
5. M. Makyta, V.D., G. M. Haarberg, J. Thonstad, *Electrodeposition of titanium diboride from fused salts.* Journal of Applied Electrochemistry, 1996. **26**(3): p. 319-324.
6. Masaya Shigeta, T.W., *Multi-component co-condensation model of Ti-based boride/silicide nanoparticle growth in induction thermal plasmas.* Thin Solid Films, 2007. **515**(9): p. 4217-4227.
7. S. Dallaire, B.C., *Plasma spray synthesis of TiB2-Fe coatings.* Thin Solid Films, 1984. **118**(4): p. 477-483.
8. I. Song, L.W., M. Wixom, and L. T. Thompson, *Self-propagating high temperature synthesis and dynamic compaction of titanium diboride/titanium carbide composites.* Journal of Materials Science, 2000. **35**(10): p. 2611-2617.
9. T. Kodama, Y.I., and H. Tamura, *Reactive Thermal Spray by High Velocity Ceramic Jet and Characterization of the Coatings.* Journal of Thermal Spray Technology, 1999. **8**(4): p. 537-544.
10. Antonio M. Locci, R.O., and Giacomo Cao, *Simultaneous Spark Plasma Synthesis and Densification of TiC–TiB2 Composites.* Journal of American Ceramic Society, 2006. **89**(3): p. 848-855.
11. Ramachandran, M., ; Reddy, R. G,, *Production of Nanoscale Titanium Diboride Powders.* Journal of Manufacturing Science and Production, 2011. **11**(1): p. 15-22.
12. P. R. Taylor, M.M.a.S.A.P. in *Proceedings of the EPD Congress, TMS Annual Meeting.* 1995. Las Vegas, Nevada: TMS.
13. G. L. Watt, G.L., ; Taylor, P. R.,; and Pirzada, S. A.,. in *Proceedings of the EPD Congress, TMS Annual Meeting.* 1995. Las Vegas, Nevada: TMS.
14. Roine, A., *HSC Chemistry 5.1.* 2002, Outokumpu Research Oy: Pori, Finland.
15. *Powder Diffraction File-4 (PDF-4).* 2011, International Centre for Diffraction Data (ICDD), Joint committee on powder diffraction Standards (JCPDS).